

# Assessing Field and Laboratory Calibration Protocols for the Diviner 2000 Probe in a Range of Soils with Different Textures

Giuseppe Provenzano, Ph.D.<sup>1</sup>; Giovanni Rallo, Ph.D.<sup>2</sup>; and Hiba Ghazouani<sup>3</sup>

**Abstract:** Frequency domain reflectometry (FDR) downhole sensors have been increasingly used for soil moisture field monitoring because they allow measurement, even continuously, along a soil profile. Moreover, they can also be installed with minimal soil disturbance around the access tube. The objectives of the paper were to assess the field and laboratory calibration protocols for a FDR capacitance probe (Diviner 2000) for a range of soils characterized by different particle size distributions and shrink/swell potential and to propose a practical and effective protocol on the basis of undisturbed soil samples, accounting for soil shrinkage/swelling processes characterizing swelling clay soils. The experiments showed that on coarse-textured soils, field calibration under wet, moist, and dry conditions allows estimations of the volumetric soil water content, with root-mean-square error (RMSE) values always lower than  $0.058 \text{ cm}^3 \cdot \text{cm}^{-3}$ . On the contrary, the problems occurring in the field on finer-textured soils, which are characterized by a clay content ranging between 36.7 and 45.1% and moderate to high shrink/swell potential, did not permit identification of suitable calibration equations and then accurate estimations of the soil water content. For such soils, in fact, a great dispersion of the experimental data and consequently high error values associated with the site-specific calibration equations, i.e., up to  $0.121 \text{ cm}^3 \cdot \text{cm}^{-3}$  for the soil characterized by the highest clay percentage, were observed. The laboratory experiments were carried out by using undisturbed soil monoliths which, compared with sieved soils, have the advantage of accounting for the natural soil structure surrounding the access tube and monitoring the soil shrinkage processes occurring in clay soils during sensor calibration experiments. The Diviner 2000 calibration equations obtained in the laboratory were characterized by error values generally lower than those obtained in the field and always smaller than  $0.053 \text{ cm}^3 \cdot \text{cm}^{-3}$ . Finally, in the range of a soil water content between approximately 10% and the maximum observed, the scaled frequency measured by the sensor was almost constant at a decreasing soil water content. This circumstance can be ascribed to the normal phase of the shrinkage process determining the compensative effects between the reduction of the volumetric soil water content and the increasing soil bulk density. The maximum variations of scaled frequency were observed in the range of the soil water content, for which the resulting soil bulk density was approximately constant. The knowledge of the soil shrinkage characteristic curve therefore assumes a key role when calibrating FDR sensors on shrinking/swelling clay soils. DOI: [10.1061/\(ASCE\)IR.1943-4774.0000950](https://doi.org/10.1061/(ASCE)IR.1943-4774.0000950). © 2015 American Society of Civil Engineers.

**Author keywords:** Frequency domain reflectometry (FDR); Capacitance probe; Soil water content; Dielectric permittivity; Shrinking/swellings soils; Calibration protocols.

## Introduction

During the last decade, frequency domain reflectometry (FDR) sensors have been largely used as equipment for indirect measurements of soil water content (SWC) because they allow, if compared with traditional methods, easy and nondestructive evaluations (Fares and Alva 2000). Mazahri et al. (2008) underlined the importance of soil moisture sensors operating in plastic access tubes inserted in the soil, i.e., downhole soil moisture sensors, for ecohydrological research and/or precision irrigation scheduling.

Compared with other soil moisture sensors, downhole sensors have the advantage of being installed with minimal disturbance of the soil around the access tube so that it is not necessary to excavate any soil pits and measuring SWC along a soil profile. However, the access tubes can be installed only in the case of soils with no rocks and/or stones.

Among the downhole FDR sensors, Diviner 2000 ([Sentek Environmental Technologies 2001](#)) is a handheld soil water content monitoring device consisting of a portable display/logger unit connected to an automatic depth-sensing probe, in which two electric rings forming a capacitor are installed at its extremity. The capacitor and the oscillator represent a circuit generating an oscillating electrical field that propagates into the soil medium through the wall of the access tube. Figs. 1(a and b) show a schematic view of the probe for field and laboratory calibration. The sensor's output is represented by the circuit resonant frequency (raw count),  $F$ , depending on the dielectric properties of the soil surrounding the access tube, which is variable in a range from approximately 240 to 330 MHz, which includes the range from approximately 250 MHz in saturated soil to approximately 287 MHz in air-dry soil (Evett et al. 2006). The Enviroscan probe ([Sentek Environmental Technologies 2001](#)) uses the same access tube, but consists of an array of identical sensors placed permanently at fixed depths and

<sup>1</sup>Associate Professor, Dipartimento Science Agrarie e Forestali, Università degli Studi di Palermo, Viale delle Scienze 12, 90128 Palermo, Italy.

<sup>2</sup>Researcher, Dipartimento Science Agrarie, Alimentari, Agro-ambientali, Università di Pisa, Via del Borghetto 80, 56124 Pisa, Italy (corresponding author). E-mail: giovanni.rallo@unipi.it

<sup>3</sup>Ph.D. Student, Département du Génie des Systèmes Horticoles et du Milieu Naturel, Institut Supérieur de Chott Meriem (ISA-CM), BP 47, Sousse 4042, Tunisie.

Note. This manuscript was submitted on January 27, 2015; approved on July 1, 2015; published online on September 2, 2015. Discussion period open until February 2, 2016; separate discussions must be submitted for individual papers. This paper is part of the *Journal of Irrigation and Drainage Engineering*, © ASCE, ISSN 0733-9437/04015040(12)/\$25.00.

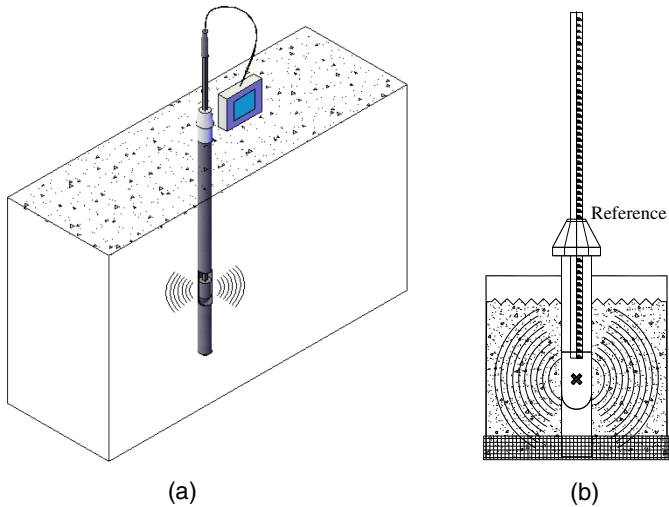


**Fig. 1.** Schematic view of Diviner 2000 probe: (a) field calibration; (b) laboratory calibration

offers the advantage of logging both the time and depth series of the soil water content.

It has been demonstrated that 99% of the sensitivity is within a radius of 10 cm from the sensor axes (Paltineanu and Starr 1997), whereas approximately half of its sensitivity depends on the soil water content in the annular region, which has a thickness ranging between 1 and 2 cm around the surface of the access tube. This last circumstance, however, makes the instruments very sensitive to inconsistencies caused by incorrect installation, resulting in air gaps beside the access tube.

The resonant frequency detected by the sensor in the soil ( $F_s$ ) is scaled to a value SF ranging between 0 and 1 on the basis of the frequency readings obtained after placing the access tube in air ( $F_a$ ) and water ( $F_w$ )

$$SF = \frac{F_a - F_s}{F_a - F_w} \quad (1)$$

The volumetric soil water content,  $\theta$  ( $\text{cm}^3 \cdot \text{cm}^{-3}$ ) can then be evaluated by solving the calibration equation, which is usually expressed as

$$SF = a\theta^b + c \quad (2)$$

where  $a$ ,  $b$ , and  $c$  = fitting parameters. Specifically for Enviroscan, the default equation initially proposed by the manufacturer and derived from an average of three different Australian soils (sand, loam, and clay loam) was characterized by  $a = 0.1957$ ,  $b = 0.404$ ,  $c = 0.0285$ , and  $R^2 = 0.974$  (Sentek Environmental Technologies 2001), where  $\theta$  is expressed as a percentage of the apparent soil volume.

Several authors have stated that the additive constant of Eq. (2) can be assumed equal to 0 (Morgan et al. 1999; Geesing et al. 2004; Groves and Rose 2004; Gabriel et al. 2010). In fact, considering that for  $\theta$  tending to 0, the corresponding SF values suddenly decrease, and, for practical applications, the related errors can be neglected. The default equation valid for Diviner 2000 was obtained under the latter hypothesis, with values of fitting parameters equal to  $a = 0.2746$  and  $b = 0.3314$  ( $R^2 = 0.9985$ ). However, the calibration equation proposed by the manufacturer cannot provide accurate measurements of the volumetric soil water content for all the soil types, considering that the soil dielectric properties are affected by the soil texture and structure. Moreover, agricultural

activities also play a significant effect on soil properties like bulk density and organic matter content, therefore affecting its water storage capacity. Site-specific calibration equations have therefore been largely recommended to obtain accurate values of the actual volumetric soil water content (Paraskevas et al. 2012; Evett et al. 2006).

In the last two decades, numerous experiments have been carried out in the field and laboratory to identify site-specific calibration equations for Enviroscan and Diviner 2000 sensors on soils characterized by different textures to evaluate the effects of soil salinity and temperature on the performance of the sensors. Among the first, Mead et al. (1995) presented the calibration and sensitivity analysis of the Enviroscan probe to salinity and bulk density changes related to three soil types: coarse sand, sandy loam with two bulk densities, and clay soil. The sensor calibration, carried out under controlled laboratory conditions, showed significant differences even within the two sandy loam soils, which only differed in bulk density. Using the Enviroscan probe and default calibration equation on three sandy soils collected in Florida, Morgan et al. (1999) observed the underestimation of the soil water content when the default calibration equation was used.

Alternatively, in shrinking/swelling clay soils, Burgess et al. (2006) carried out a comparison between the Diviner 2000 and the neutron probe. These authors indicated that the site-specific calibration equations obtained for both sensors were substantially different from the default equation even if, after a field calibration, the two instruments gave similar estimates of change in the soil water content integrated over a meter depth. Even Gabriel et al. (2010), on the basis of field and laboratory measurements with the Enviroscan probe on loamy soils, determined calibration equations that were characterized by satisfactory coefficients of determination,  $R^2 = 0.96$  and 0.92, respectively, whose fitting parameters, however, were significantly different than those characterizing the default equation.

On the basis of experimental data acquired on laboratory columns filled with three different soils, i.e., silt loam, loam, and clay, Evett et al. (2006) obtained calibration equations for Diviner 2000 and Enviroscan that were characterized by a high coefficient of determination ( $R^2 > 0.99$ ) and a RMSE on the order of  $0.02 \text{ cm}^3 \cdot \text{cm}^{-3}$ , even if in a previous field calibration of Diviner 2000 on two Austrian soils (silty clay loam and silt loam), Evett et al. (2002) presented a lower  $R^2$  ( $R^2 = 0.533$  and 0.416) and higher RMSE (RMSE = 0.038 and 0.046).

According to Paltineanu and Starr (1997), the accuracy of the field calibration equation depends on errors related to the sampling of the soil volume investigated by the sensor, which must be done accurately. Moreover, in swelling/shrinking soils, the changes of soil bulk volume with the soil water content cause a modification in the pore geometry, as indicated by the bulk density–soil water content relationship (soil shrinkage characteristic curve). The coefficient of linear extensibility (COLE) (Grossmann et al. 1968; Franzmeier and Ross 1968), which is derived by the bulk densities of soil clods or undisturbed samples, is generally used for quantifying soil shrink/swell potential. The higher the presence of clay minerals in the smectite group, the greater the soil shrink/swell potential, whereas illitic clays manifest intermediate shrink/swell potential and kaolinitic clays are least affected by volume changes with the soil water content.

Malicki et al. (1996) and Davood et al. (2012) suggested that the changes in soil bulk density must not be disregarded when calibrating capacitance sensors. Even Fares et al. (2004), on the basis of field experiments, estimated errors in the volumetric soil water content of up to 20% when ignoring the variations of soil bulk density.

On the contrary, on the basis of laboratory experiments aimed to calibrate the ThetaProbe Type ML1 (Delta-T Devices, Cambridge,

U.K.) on a clay loam soil, Lukunu and Savage (2006) observed a negligible influence of the variations of clay content, soil bulk density, and soil temperature detected at different investigation depths on the measured soil water content. Actually, soil bulk density has to be considered a source of uncertainty in volumetric soil water content estimation because it influences soil dielectric permittivity (Gardner et al. 1998) and governs the relationship between gravimetric and volumetric soil water contents (Geesing et al. 2004).

Hignett and Evett (2008) underlined that the default calibration equation has to be performed in a temperature-controlled room by using distilled water and homogeneous soil materials, i.e., loams or sands that are uniformly packed around the sensor. Even if the suggested procedure was addressed to a very accurate calibration, the resulting equation cannot be extended to common field conditions.

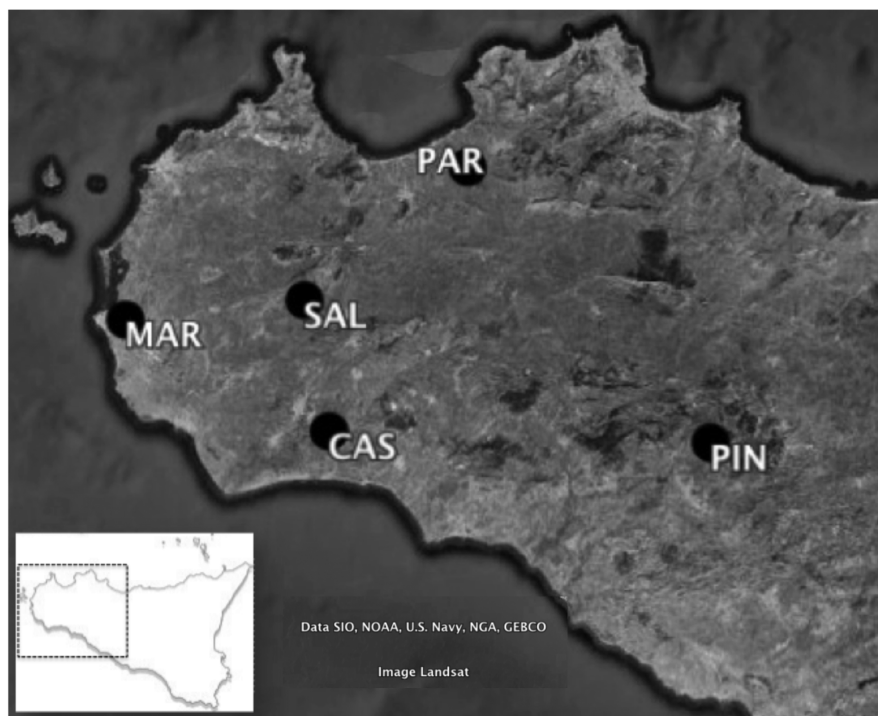
Despite the manufacturer's recommendation to use the default calibration equations to monitor the "relative soil water status," the need for site-specific calibration arises when the actual soil water content is monitored for irrigation scheduling (Evett et al. 2011). The review of Robinson et al. (2008) has recently proposed consideration of soil water content as an environmental variable, which should be monitored and shared in common databases aimed to assume a global awareness of different water-controlled phenomena. With this in mind, the actual values of the soil water content have to be considered so that when using a certain sensor, it is crucial to achieve its highest accuracy.

Moreover, the need to standardize methodologies and techniques for laboratory and field calibration of electromagnetic (EM) soil water sensors has been recently emphasized by Paltineanu (2014) during the Fourth International Symposium on Soil

Water Measurement Using Capacitance, Impedance and Time Domain Transmission (TDT), which was held in Montréal. Experimental protocols for the calibration of any soil water content sensor must provide detailed information describing the sensor's physical response to the system, e.g., operation frequency, response to air and distilled water at approximately 22°C, room temperature, and axial and radial sensitivity of the sensor in distilled water in air-water and air-soil interfaces; and the soil intrinsic characteristics, e.g., texture, clay mineralogy, electrical conductivity, organic matter, gravel content, and coefficient of uniformity for bulk density in the soil volume investigated by the sensor. Additionally, the common use of statistical analysis and data interpretation was finally advocated. Even if copious literature exists on FDR sensor calibration for different soils, the lack of a site-specific calibration equation for Sicilian soils, for which other research is ongoing (Cammalleri et al. 2013; Provenzano et al. 2013; Rallo et al. 2012, 2014), and the requirements of standardizing the calibration protocols indicated the need to pursue the following objectives: (1) to assess field and laboratory protocols to calibrate a Diviner 2000 capacitance probe on seven irrigated soils of Western Sicily that are characterized by a different texture and shrink/swell potential; and (2) to analyze their performance and propose a practical and effective protocol of sensor calibration on the basis of undisturbed soil samples.

## Materials and Methods

Experiments were carried out on seven different soils collected in the five irrigated areas of Western Sicily shown in Fig. 2, which are



Site	ID	UTM ED50 coordinates [m]	
		East	North
Partinico (PA)	PAR	330516.8	4208994.2
Castelvetrano (TP)	CAS	310086.4	4168408.9
Marsala (TP)	MAR	278561.3	4186111.9
Pietranera (AG)	PIN	367878.4	4165752.0
Salem (TP)	SAL	305920.6	4188651.2

**Fig. 2.** Map and localization of investigated sites (map data: Google, SIO, NOAA, U.S. Navy, NGA, GEBCO, Landsat)

representative of different textural classes. Sampling sites were chosen according to the variability of soil particle distribution and contained a limited gravel content, low salinity, and low amount of organic matter. For the site of Castelvetrano (CAS), two different locations were investigated: the first, CAS-A, was located in an area characterized by a coarse-textured soil, whereas the second was located in an area with a higher clay content. For the latter, two different soil layers, i.e., 0–30 and 60–90 cm, were investigated: CAS-B and CAS-C.

Disturbed soil samples were used for the preliminary particle size analysis and to evaluate the gravel content and soil electrical conductivity. Particle size distribution was determined by coupling a sieving column and the Bouyoucos hydrometer (ASTM 152H, H-B Instrument Company, U.S.). The textural classes were defined according to the USDA classification system (Soil Survey Division Staff 1993). For each soil sample, the amount of skeleton ( $\text{g} \cdot \text{kg}^{-1}$ ) was determined by dividing the weight (g) of the material held by a 5-mm sieve to the dry weight (kg) of the original sample from which it was extracted (Pagliai 1998). The retained material was washed with a Calgon solution (sodium hexametaphosphate) dried in an oven at 105°C for 48 h and finally weighted.

The soil electrical conductivity, EC, was determined on the soil-water extract 1:5 with a conductivity meter (microCM 2200, Crison Instruments, Barcelona) by following the standard procedure presented by Pagliai (1998). For each site, the calibration equation for the Diviner 2000 capacitance probe was determined by following the standard field procedure, as suggested in the user's manual, and using a laboratory procedure on undisturbed soil samples, as described in detail in the following.

### Field Calibration

Field calibration took place in 2013 during measurement campaigns carried out in three different periods of the year, with the aim to explore a relatively wide domain of soil water contents, i.e., wet, moist, and dry. The first measurement campaign was generally carried out after significant rainfall events so that the soil water status was approximately close to the field capacity. The second campaign was accomplished when soil water contents ranged between 0.15 and 0.25  $\text{cm}^3 \cdot \text{cm}^{-3}$ , whereas the third was completed at the end of the dry season for soil water contents lower than approximately 0.15  $\text{cm}^3 \cdot \text{cm}^{-3}$ .

For each selected site, six polyvinyl chloride (PVC) access tubes with a length of 0.35 m were installed in three groups consisting of two that were investigated in pairs during each measurement campaign. To avoid interference, the distance between each group of access tubes was 0.30 m, whereas the distance between the pairs was 0.50 m. Access tubes were installed with the specific kit to reduce soil disturbance during installation and ensure perfect contact between the soil and tube to avoid air gaps and preferential water flow.

During each measurement campaign, the values of SF were initially acquired by placing the sensor in the air and in water and then in both the access tubes, with a 5-cm step, from 5- to 25-cm depths. To reduce the measurement errors, scaled frequencies were acquired during the descent and ascent of the sensor into the tube and then averaged at each single depth. After the measurements, 12 undisturbed soil samples (8.0-cm diameter and 5.0-cm height) at four distinct soil depths (0–5, 5–10, 15–20, and 25–30 cm) were collected around each access tube. Immediately after collection, soil samples were leveled, cleaned, and weighed, with an accuracy of balance of 0.01 g. Samples were then oven dried at 105°C for 48 h, weighted, and finally sieved to determine the skeleton content, gravimetric water content, soil bulk volume, and, finally,

volumetric water content for each of them. The values of soil bulk volume were corrected to account for the amount of skeleton identified in the sample, as suggested by Cavazza (2005).

### Laboratory Calibration

Laboratory calibration was carried out on undisturbed soil monoliths that have a diameter and height equal to approximately 0.25 m, in which contemporary measurements of SF, gravimetric soil water content ( $U$ ), and the corresponding soil bulk density  $\rho_b$  were carried out to cover the range from field capacity to oven dry. The dimensions of soil samplers were chosen according to the sensing volume investigated by the sensor so that approximately 99% of the sensor response was controlled by the soil inside the monolith.

For all of the investigated sites, two samples were collected after extensive rainfall events when the soil water content was close to field capacity to avoid rewetting the soil before starting the experiment. The photographic sequence in Figs. 3(a–i) shows the different phases of sampling. The soil surface was leveled [Fig. 3(a)] before inserting a 0.30-m-long access tube. To ensure verticality, a wood guide and level were used during installation [Figs. 3(b–d)]. Once installed [Fig. 3(e)], the access tube was cleaned inside and the sampler was positioned in a way to set the access tube in its axial position [Fig. 3(f)]. A hammer was used to gradually tap the sampler in the soil [Fig. 3(g)]. Finally, the soil sample was carefully removed [Figs. 3(h and i)], wrapped in a plastic film, sealed, and transported to the laboratory. The scaled frequency and corresponding weight of the sample were measured during an air-drying process, initially on a daily frequency, which was later reduced according to the water lost.

At the same time, the apparent volume of the soil monolith was monitored to consider the possible shrinking processes characterizing the soils containing swelling clay (Crescimanno and Provenzano 1999). Vertical subsidence of the soil surface was measured on eight marked positions chosen along two orthogonal directions, with a precision Vernier caliper (accuracy of 0.1 mm) bolted to a bar, allowing bidimensional movements. A microswitch glued to the shaft of the caliper was activated by contact with the soil surface. For each soil water content, the sample height was then obtained by considering the arithmetic mean of the eight values. The sample was then oven dried, and finally its weight and height were remeasured. After oven drying, the PVC sampler was removed and the circumference of the core was measured with a flexible tape (accuracy of 0.5 mm) at three different heights.

The latter measurement allowed the determination of the geometrical factor (Bronswijk 1990), which was assumed valid for the whole shrinking process, which accounts for the relative amount of vertical contraction caused by the change of the sample volume. On the basis of these measurements, it was possible to determine the soil bulk volume corresponding to each measured gravimetric water content, soil bulk density, and, finally, volumetric water content.

The knowledge of soil bulk volumes at field capacity,  $V_{\text{wet}}$ , and after oven drying,  $V_{\text{dry}}$ , allowed quantification of the shrink/swell potential of the investigated soils according to COLE, which was evaluated as (Grossman et al. 1968)

$$\text{COLE} = \left( \frac{V_{\text{wet}}}{V_{\text{dry}}} \right)^{1/2} - 1 \quad (3)$$

### Statistical Analysis

The knowledge of volumetric water contents and the corresponding scaled frequencies allowed fitting of the calibration equation,

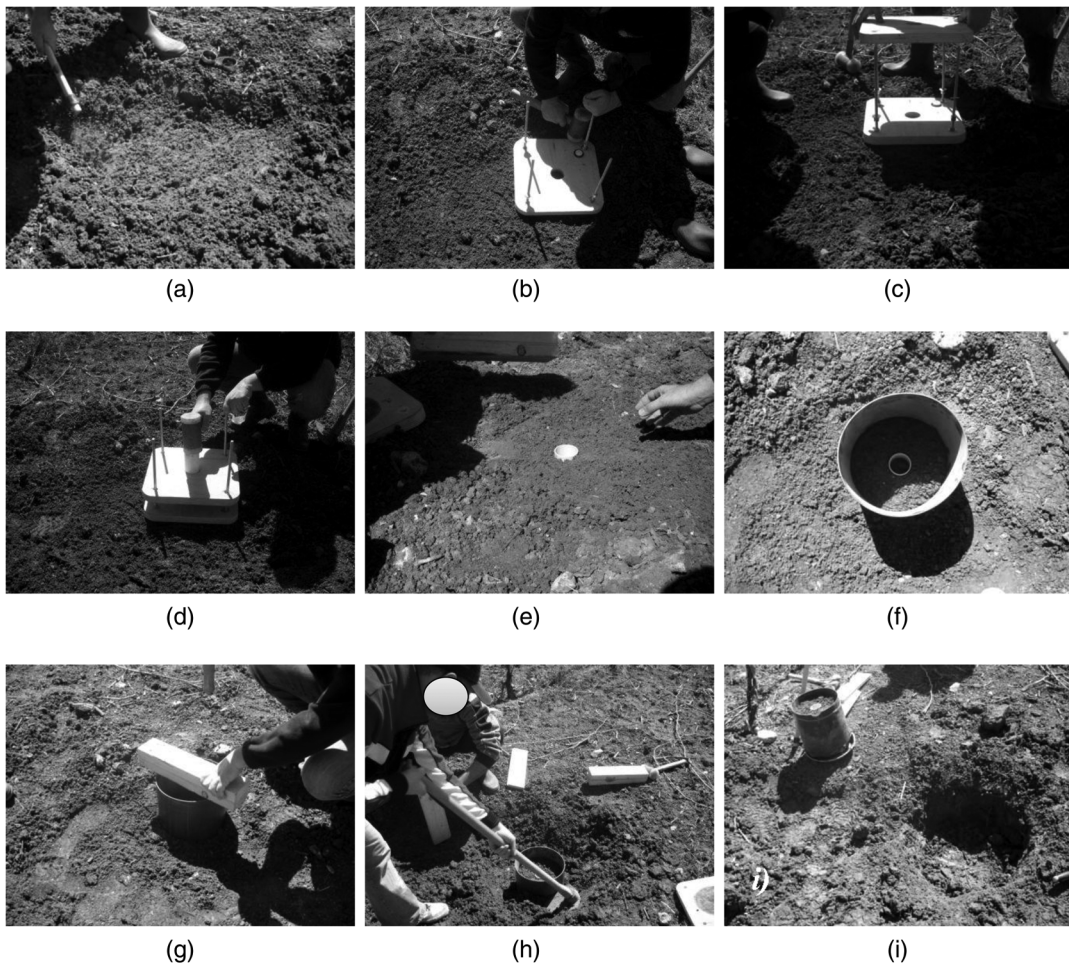


**Fig. 3.** Steps for collecting undisturbed soil monoliths

which is represented by the exponential regression of Eq. (2), assuming  $c = 0$ . According to Geesing et al. (2004), even though SF is the dependent variable, it was considered the independent variable because the equation application is aimed to derive the volumetric water content  $\theta$  from the scaled frequencies SF provided by the sensor. The exponential regression was obtained on both field and laboratory data using *SYSTAT 13* for nonlinear regression, whose output also provides  $R^2$  and RMSE.

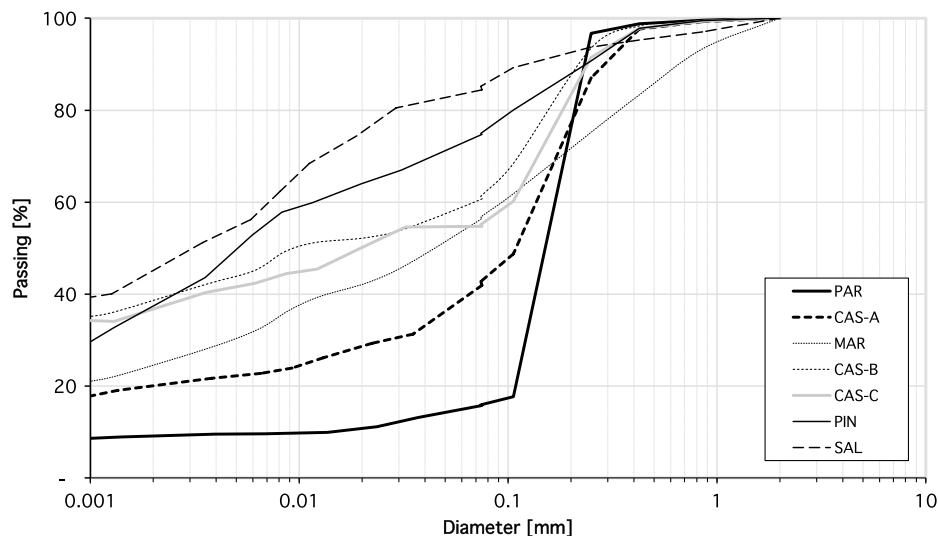
## Results and Discussion

Fig. 4 shows the particle size distributions for the examined soils, indicating the extremely high variability that characterizes them. Table 1 summarizes the percentage of clay, silt, sand, and soil textural class (Soil Survey Division Staff 1993), content of the skeleton, percentage of organic matter (OM), and values of soil electrical conductivity ( $EC_{1.5}$ ). As can be observed, according to the clay and sand contents, whose values ranged from 9.1 to 45.1% and 17.3 to 85.8%, respectively, the soils cover different textural classes. According to the percentage of the skeleton, which is variable between 2 and  $72\text{ g} \cdot \text{kg}^{-1}$ , samples can be considered very slightly ( $<30\text{ g/kg}$ ) or slightly stony ( $30\text{--}150\text{ g/kg}$ ) (Boden 1994). On the basis of  $EC_{1.5}$ , which ranged from 0.11 and 0.36  $\text{dS} \cdot \text{m}^{-1}$ , soils can be classified as nonsaline (Soil Survey Division Staff 1993).

## Field Calibration

For the different sites, Fig. 5 shows the average values of the measured volumetric soil water content,  $\theta$ , as a function of SF measured in the field. The error bars identify the standard deviations of  $\theta$ , obtained by considering the three undisturbed samples collected at the same depth. Fig. 5 also illustrates the  $\theta(\text{SF})$  relationships suggested by the manufacturer and the experimental regression curves, fitted according to Eq. (2), whose coefficients and statistical parameters, indicated in Table 2, were obtained assuming the condition of  $c = 0$ , despite the slight regression improvement associated with an intercept different than zero (Paltineanu and Starr 1997). Table 2 also indicates the ranges of variability of measured soil water contents and RMSE values associated with both of the fitting regression curves and the default calibration equation.

As can be observed in Fig. 5, for the three coarser-textured soils PAR, CAS-A, and MAR, despite the relatively high dispersion of the experimental data, the empirical  $\theta(\text{SF})$  relationships obtained in the field were very close to the one proposed by the manufacturer, as demonstrated by the similar RMSE values indicated in Table 2. The relatively good performance associated with the default equation ( $\text{RMSE} \leq 0.08\text{ cm}^3 \cdot \text{cm}^{-3}$ ) confirms the general validity of this equation for coarse-textured soils, even if the site-specific calibration equation gets to a general improvement of soil water content estimations. On the contrary, for the finer-textured soils CAS-B, PIN, and SAL, it was not possible to determine reliable calibration equations, primarily because of soil cracking observed in the field.



**Fig. 4.** Particle size distribution obtained on investigated soils

**Table 1.** Physical Properties of Investigated Soils

Site	Identifier	Clay (%)	Silt (%)	Sand (%)	Soil textural class (USDA)	Skeleton ( $\text{g} \cdot \text{kg}^{-1}$ )	OM (%)	$\text{EC}_{1:5}$ ( $\text{dS} \cdot \text{m}^{-1}$ )
Partinico	PAR	9.1	5.1	85.8	S-L	20	ND	0.11
Castelvetrano	CAS-A	20.0	16.3	63.7	L-S-C	17	2.0	0.31
Marsala	MAR	24.6	26.9	48.5	L-S-C	32	2.6	0.22
Castelvetrano	CAS-B	38.7	13.4	42.4	L-C	4	1.9	0.18
Pietranera	PIN	37.4	33.8	28.8	L-C	32	2.0	0.35
Castelvetrano	CAS-C	36.7	17.9	45.3	S-C	2	2.0	0.18
Salemi	SAL	45.1	37.6	17.3	C	72	2.0	0.23

Note: ND = determined.

The occurrence of shrinking processes in the finer-textured soils could have determined the opening of cracks in the soil volume investigated by the sensor even during the second measurement campaign. This circumstance was particularly evident for the soil PIN, for which the loss of contact between the soil and access tube was visible with the naked eye when the soil was dry, making it impossible to collect any consistent data. For this soil, therefore, despite the high  $R^2$  ( $R^2 = 0.87$ ) and low RMSE (RMSE = 0.042) obtained, considering the limited number of reliable data acquired, the fitted equations cannot be considered appropriate for the whole range of SWCs occurring in the field.

A different problem took place in the CAS-C site, where, in relation to the investigated soil layer (60–90 cm), the variations of the soil water content were quite limited, with values that never decreased below 20%. A similar behavior was observed by Fares et al. (2004) on a clay subsoil, in which the minimum soil water content measured in the field was equal to 18.3%. In this case, it was not possible to identify a calibration equation valid for a wide range of soil water contents.

For the three coarser-textured soils, the default calibration equation generally underestimates the measured volumetric water content when the scaled frequency assumes values lower than approximately 0.85 and overestimate  $\theta$  in other cases. Geesing et al. (2004) and Polyakov et al. (2005) observed that the default calibration equation generally overestimates  $\theta$  on a silt-loamy soil and silty-clay-loam and clay-loam soils, respectively. According to the RMSE values associated with the default calibration equations indicated in Table 2, it is noteworthy that in finer-textured soils, the

values of RMSE tend to increase at an increasing clay content, reaching values even higher than  $0.10 \text{ cm}^3 \cdot \text{cm}^{-3}$ .

Fig. 6 shows the values of  $\rho_b$  and  $U$  determined on soil cores collected around the access tubes as a function of sampling depth. As it can be noticed, the average bulk density, increasing at an increasing depth in the layer 0–30 cm, is, in general, characterized by a greater variability in the top layers compared with the deeper layers. Moreover, for each fixed depth, a quite high variability is also evident on the gravimetric water content. Even Paltineanu and Starr (1997) underlined the great variability associated with both the soil bulk density and gravimetric water content, making it difficult, therefore, to obtain low RMSE values in the field. The spatial variability observed on  $\rho_b$  and  $U$  could be associated with the sampled soil volume, which is not representative of the fringe volume investigated by the sensor, whereas the temporal variability can be a consequence of the different soil bulk density with the soil water content at sampling, which is associated with the presence of swelling clays. Similar results were found by Paltineanu and Starr (1997) who discussed the difficulties of getting accurate field measurements of  $\rho_b$  and  $\theta$  in the fringe volume investigated by the sensor, indicating that more accurate calibration equations can be obtained under more controlled laboratory conditions, where it is possible to minimize the uncertainties associated with the field measurements.

### Laboratory Calibration

Since the publication of the manufacturer's user manual (Sentek Environmental Technologies 2001), several investigations have

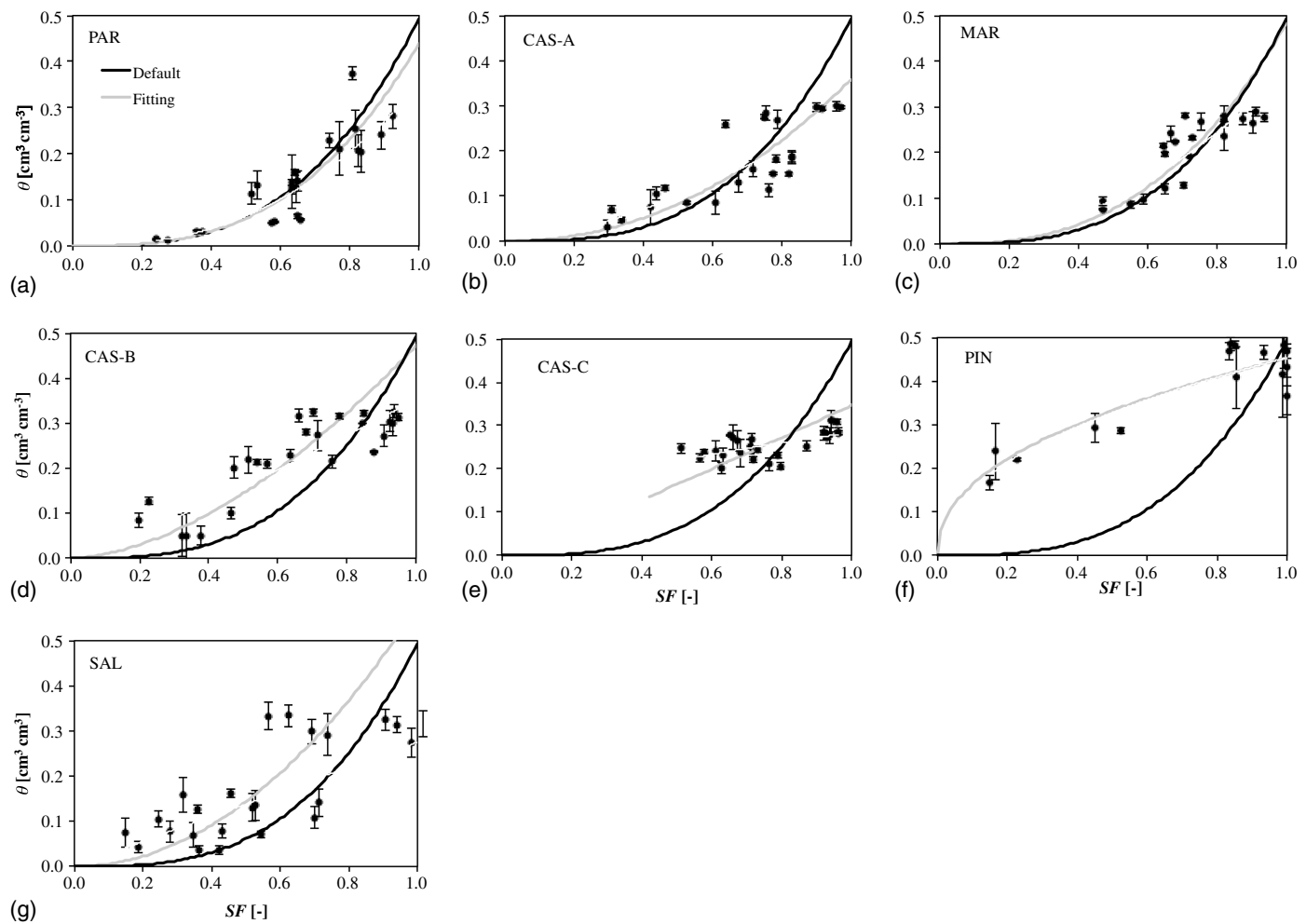


**Fig. 5.** Volumetric soil water content,  $\theta$ , SF, and data pairs measured in the field on different soils in three experimental measurement campaigns; error bars indicate standard deviations of measured  $\theta$ ; fitting regressions and default calibration equation are also shown

**Table 2.** RMSE Associated with the Fitting Regressions and Default Calibration Equations

Identifier	Range of $\theta$ ( $\text{cm}^3 \cdot \text{cm}^{-3}$ )			Fitting regression equation			Default equation	
	N	Minimum	Maximum	a	b	$R^2$	RMSE	RMSE ( $\text{cm}^3 \cdot \text{cm}^{-3}$ )
PAR	24	0.01	0.37	0.439	2.869	0.84	0.049	0.054
CAS-A	24	0.03	0.30	0.359	2.130	0.76	0.054	0.080
MAR	18	0.08	0.29	0.482	2.650	0.73	0.058	0.063
CAS-B	24	0.05	0.33	0.473	1.709	0.67	0.074	0.100
PIN	16	0.17	0.49	0.453	0.446	0.87	0.042	0.166
CAS-C	27	0.20	0.31	0.347	1.084	0.35	0.040	0.110
SAL	24	0.04	0.33	0.576	2.007	0.49	0.121	0.113

Note: The number of measurements, range of  $\theta$ , and parameters of Eq. (2) are also indicated for the different soils.

been carried out regarding FDR sensors under laboratory conditions. Paltineanu and Starr (1997), Gabriel et al. (2010), Haberland et al. (2014), and Rallo and Provenzano (2014) presented site-specific calibration equations obtained on soil samples prepared in the laboratory by using soils with different textures and sieved through a 5-mm mesh.

The laboratory calibration procedure proposed in this paper refers to undisturbed soil monoliths to account for the natural soil structure surrounding the access tube and the possible variations of the apparent soil volume because of the presence of swelling clay. Using such monoliths in fact allows the contextual monitoring

of  $U$ ,  $\rho_b$ , and SF during an air-drying process of the soil sample. Using an undisturbed monolith represents a substantial improvement of the field calibration method listed previously.

For the different examined soils, Table 3 shows the maximum gravimetric water content measured immediately after sampling,  $U_{\max}$ , minimum and maximum bulk density ( $\rho_{b,\min}$ ,  $\rho_{b,\max}$ ), COLE, and the skeleton content S. Minimum  $\rho_b$  corresponds to the maximum soil water content at sampling and is approximately equal to field capacity, whereas maximum  $\rho_b$  corresponds to the oven-dry condition. According to the COLE values, the investigated soils showed a shrink/swell potential that ranged from low (COLE < 0.03) to high

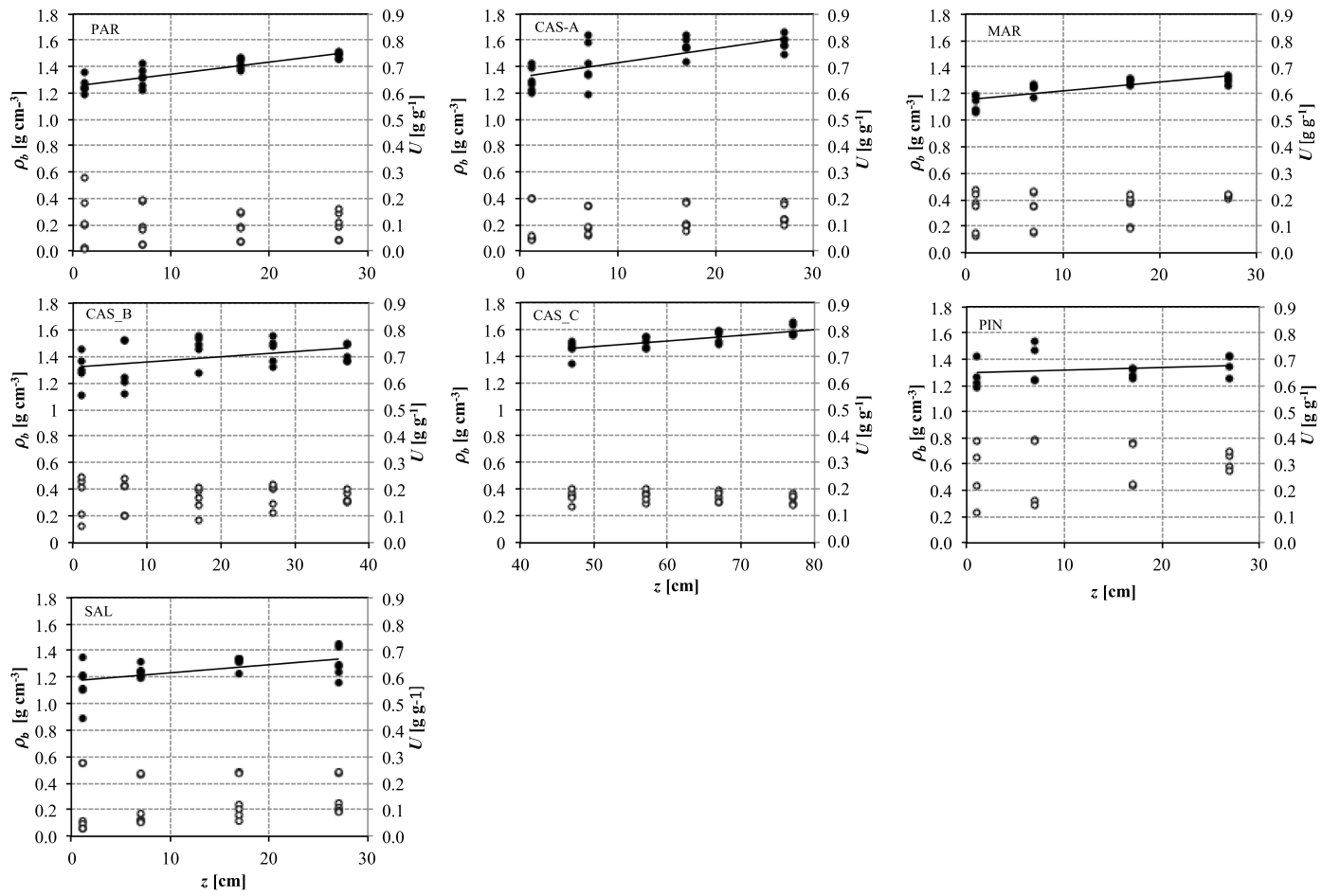


**Fig. 6.** Values of soil  $\rho_b$  (black dots) and corresponding  $U$  (white dots) measured on undisturbed soil samples ( $8.0 \times 5.0$  cm) as function of soil depths

( $0.06 < \text{COLE} < 0.09$ ) (Parker et al. 1977). Similar to that determined on smaller samples ( $8.0 \times 5.0$  cm), on the basis of the skeleton content, the considered soils are very slightly or slightly stony.

The ratio between the highest and lowest bulk density, associated with the maximum variations of soil bulk volume, varied from values slightly higher than 1.0 on coarse-textured soils to 1.25, which was obtained on the sample SAL, containing the highest clay percentages. Moreover, it is noteworthy that this ratio and the COLE values tend to increase at an increasing clay content, confirming the presence of swelling clay in the samples. As known, in fact, a value of the ratio equal to 1.0 is typically associated with rigid soils, whereas higher values are usually obtained on shrinking soils.

**Table 3.** Values of  $U_{\max}$ ,  $\rho_{b,\min}$ ,  $\rho_{b,\max}$ , COLE, and  $S$  Measured on Undisturbed Soil Monoliths

Identifier	$U_{\max}$ ( $\text{g} \cdot \text{g}^{-1}$ )	$\rho_{b,\min}$ ( $\text{g} \cdot \text{cm}^{-3}$ )	$\rho_{b,\max}$ ( $\text{g} \cdot \text{cm}^{-3}$ )	$(\rho_{b,\max}) /$ $(\rho_{b,\min})$	COLE	$S$ ( $\text{g} \cdot \text{kg}^{-1}$ )
PAR	0.28	1.50	1.51	1.00	0.000	20
CAS_A	0.27	1.40	1.49	1.06	0.020	21
MAR	0.29	1.31	1.33	1.01	0.003	32
CAS_B	0.17	1.57	1.74	1.11	0.035	4
PIN	0.21	1.40	1.70	1.21	0.066	10
CAS_C	0.20	1.41	1.65	1.17	0.054	3
SAL	0.24	1.32	1.65	1.25	0.077	72

For the different soils, Fig. 7 shows the values  $\theta$ , SF obtained on both of the monoliths, and the corresponding fitting regression curves, whose coefficients and statistical parameters, i.e.,  $R^2$  and RMSE, are indicated in Table 4. As can be noticed in Fig. 7, a limited dispersion of experimental points around the fitting curve was found only for the finer-textured soils and was practically absent for the others, which is confirmed by an  $R^2$  higher than 0.84 and RMSE values always lower than  $0.053 \text{ cm}^3 \cdot \text{cm}^{-3}$ .

Moreover, for the finer-textured soils and at the highest SF values, significant variations of  $\theta$  corresponded to limited changes of SF. This circumstance can be ascribed to the effects of increasing bulk density observed at a decreasing water content on the soil dielectric permittivity. In fact, primarily during the initial phase of the drying process, any reduction of soil porosity changes the mutual proportions of water, air, and solid particles, affecting the soil dielectric permittivity and consequently  $F_s$  detected by the sensor. As observed by Davood et al. (2012), for a fixed water content, a positive linear relationship between soil dielectric permittivity and soil bulk density exists as a consequence of the higher mass of solid particles per unit soil volume. In other terms, the almost constant SF values depend on the combined effect between the reduction of the soil water content and the contextual increase of soil dielectric permittivity. Other possible explanations for this behavior were provided by Evett et al. (2008), who referred to how capacitance sensors are influenced by some properties of the soil-water system around the access tube and not only by the water content. Such properties have been related to the soil structure and nonuniform

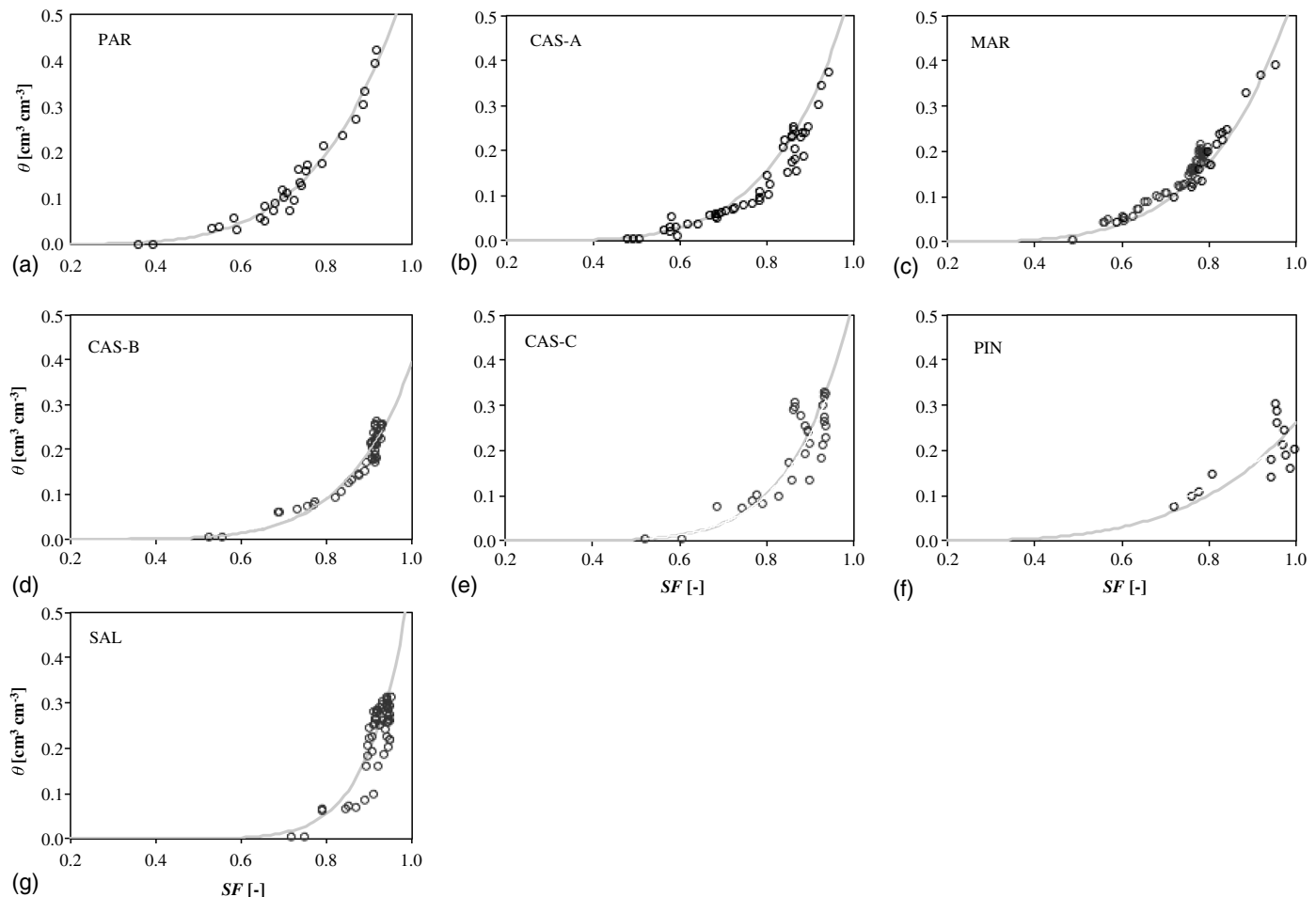


**Fig. 7.** Relationship between SF and volumetric soil water,  $\theta$ , measured on undisturbed soil monoliths and related fitting equation

penetration in the soil of the electromagnetic field generated by the sensor (Evett and Steiner 1995), the distortion of the electromagnetic field generated by the individual arrangement of soil pedes, and by the pattern of the water content in the pedes around the access tube.

To exclude the effects of variations of bulk density on the volumetric soil water content, SF values were then represented as a function of  $U$  rather than  $\theta$ . For the different soils, Fig. 8 shows the values of scaled frequency SF (main axes) as a function of  $U$  and  $\rho_b$  (secondary axes) as a function of soil bulk density obtained on both of the monoliths. As known, the relationship  $\rho_b(U)$  represents the soil shrinkage characteristic curve. By observing Fig. 8, it can be noticed that the resulting values of soil bulk density

were quite different among the soils, which particularly manifested a quite dissimilar behavior and exhibited, in several cases, extensive variations of  $\rho_b$  in the range of investigated  $U$  as a consequence of the shrinking processes that occurred in the samples.

Except for the coarse-textured soils, i.e., PAR, CAS-A, and MAR, which were characterized by the absence or limited soil shrinkage (COLE < 0.03), for the other samples, very limited variations of SF occurred in the range of gravimetric soil water contents higher than a certain threshold value ( $U^* \approx 0.10 \text{ g} \cdot \text{g}^{-1}$ ). This threshold roughly represents the lower limit of the normal phase of the shrinking process, in which the variations of soil bulk volume are approximately proportional to the gravimetric water content  $U$ . For a gravimetric water content smaller than the threshold, it can be noticed that the variations of soil bulk density are limited or absent (residual phase of the soil shrinkage characteristic curve), and, at the same time, the most significant variations of sensor-scaled frequency occur.

Similarly to that observed on the  $\theta(SF)$  experimental data pairs for finer-textured soils, even the  $SF(U)$  data showed analogous behavior, considering that SF values tend to rapidly increase at a rising  $U$  only in correspondence with the residual phase of the shrinking process ( $U < U^*$ ;  $\rho_b = \text{constant}$ ); otherwise, variations of SF tend to gradually reduce at an increasing  $U$  during the normal phase of the shrinkage process [ $U > U^*$  and  $\rho_b = f(U)$ ] up to being absent at the highest water contents.

In fact, soil contraction determines the changes in bulk soil permittivity,  $\varepsilon_b$ , depending on the rates of water, air, and solid matrix in

**Table 4.** Coefficients  $a$  and  $b$  of Eq. (2) and Related  $R^2$  and RMSE Obtained on Undisturbed Monoliths

Identifier	$N$	$a$	$b$	$R^2$	RMSE ( $\text{cm}^3 \cdot \text{cm}^{-3}$ )
PAR	38	0.607	5.013	0.94	0.029
CAS_A	45	0.571	5.813	0.93	0.015
MAR	52	0.555	5.127	0.95	0.030
CAS_B	29	0.393	6.590	0.95	0.039
PIN	16	0.282	5.152	0.94	0.044
CAS_C	30	0.534	7.310	0.87	0.053
SAL	59	0.587	10.493	0.84	0.049

Note: The total number of experimental determinations,  $N$ , on both the samples is also indicated.

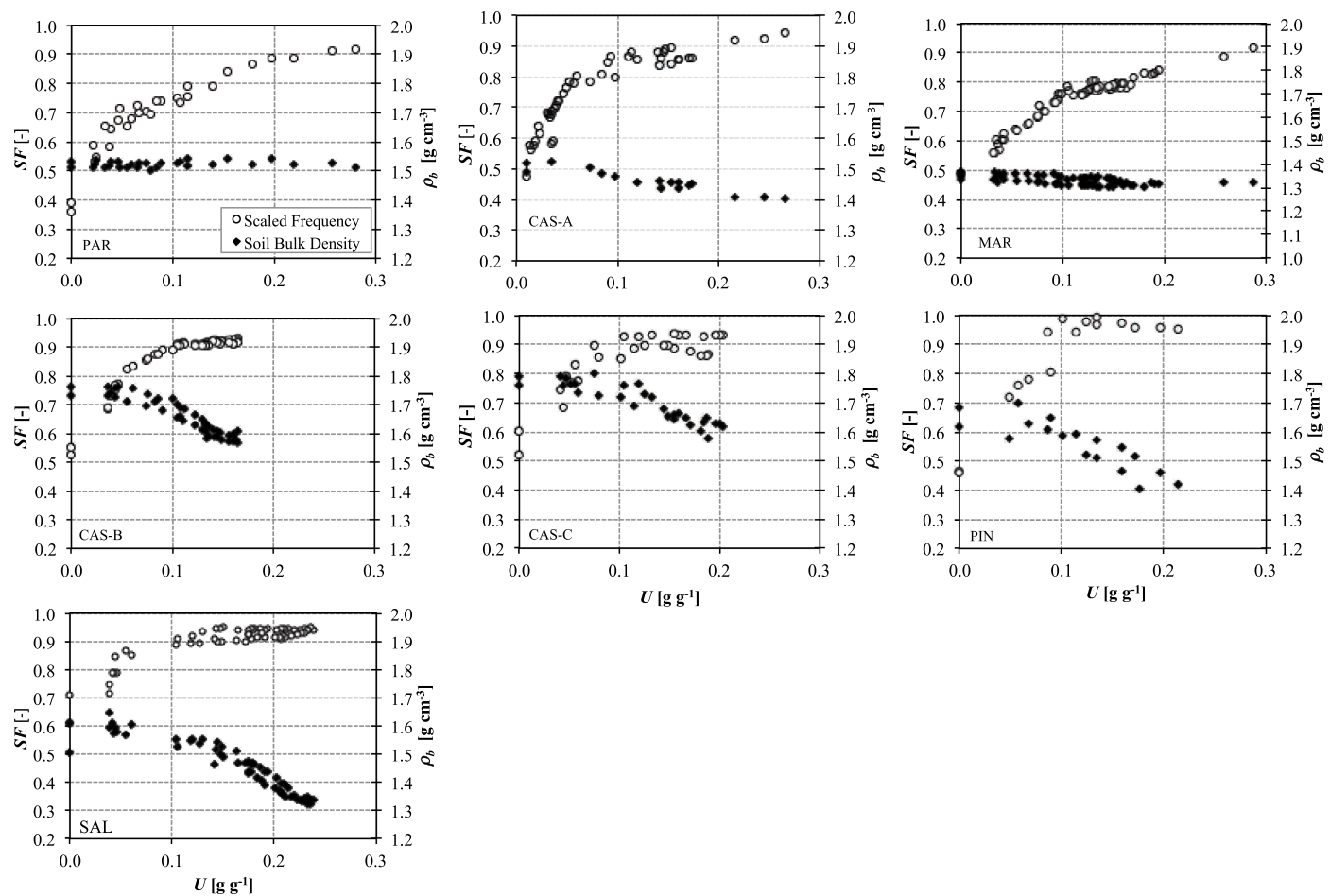


**Fig. 8.** Relationship between SF,  $U$  (white dots), and  $\rho_b$  (black dots) measured on undisturbed soil monoliths

the fringe volume investigated by the sensor. At the beginning of the shrinkage process, the relatively small reduction of SF at decreasing  $U$  can be attributed to the circumstance that the variations in the water content are in whole or in part compensated by the changes of soil bulk density. In other words, as shown by Gong et al. (2003) and more recently by Davood et al. (2012), this behavior is caused by the increase of the solid particles per unit of soil volume and consequently by the higher contribution of the soil permittivity because the solid particles are characterized by values of a dielectric constant higher than air.

## Conclusions

In this paper, field and laboratory calibration equations for the Diviner 2000 capacitance probe were assessed and a practical and effective protocol for sensor calibration was proposed. The experiments considered seven Sicilian irrigated soils characterized by different texture classes and shrink/swell potentials, a quite limited content of the skeleton, and low values of soil electric conductivity.

The results of the field calibration, which was carried out by using the procedure suggested by the manufacturer under wet, moist, and dry conditions, indicated that for the three coarser-textured soils, the default calibration equation can be considered valid, resulting in RMSE values associated with an estimated volumetric soil water content,  $\theta$ , always lower than  $0.080 \text{ cm}^3 \cdot \text{cm}^{-3}$ . However, for these soils, the site-specific calibration equation

improved the estimation of  $\theta$ , as confirmed by the systematic reduction of RMSE to values always lower than  $0.058 \text{ cm}^3 \cdot \text{cm}^{-3}$ .

For the finer-textured soils, some problems instead occurred in the field during the sensor calibration because of the presence of swelling clays, making the field calibration unreliable for these soils. In fact, soil shrinkage processes occurring under the driest examined condition and visibly evident for the soil PIN determined the opening of cracks and the presence of air gaps in the fringe volume investigated by the sensor. The loss of contact between the soil and access tube made it impossible to collect any consistent data to be used for sensor calibration. Otherwise, in the site CAS-C, because of the investigated soil depth (60–90 cm), it was possible to only explore a limited range of soil water contents of between approximately  $0.20$  and  $0.30 \text{ cm}^3 \cdot \text{cm}^{-3}$ . For finer-textured soils, RMSE values associated with the site-specific calibration equation were generally high, with values of up to  $0.121 \text{ cm}^3 \cdot \text{cm}^{-3}$  for the site SAL, characterized by the highest clay percentage. The great dispersion of  $\theta$ (SF) data pairs not only resulted as a consequence of changes in the soil water content, but also from the observed spatial and temporal variability of soil bulk density in the fringe volume investigated by the sensor. In line with Paltineanu and Starr (1997), therefore, more controlled laboratory conditions for sensor calibration allow minimization of the recognized uncertainties associated with the field measurements. Moreover, compared with a tedious and time-consuming field calibration procedure, it is possible to explore, with continuity, a wide range of soil water contents in the laboratory.

Laboratory calibration was carried out on undisturbed soil monoliths that have the advantage of accounting for the natural soil structure compared with the traditionally considered sieved samples. For shrinking/swelling clay soils, using undisturbed soil monoliths allows monitoring of the increasing bulk density at a decreasing soil water content and limiting the presence of air gaps between the access tube and the surrounding soil, which occurred in the field.

For the considered soils, it was observed that the ratio between the highest and lowest bulk density, corresponding to the oven-dry condition and maximum water content, respectively, ranged between 1.0, measured on the rigid sandy-loam soil (PAR), and 1.25, obtained on the shrinking clay soil (SAL), with values basically increasing at an increasing clay content. With the laboratory calibration protocol, compared with the field procedure, it was possible to limit the dispersion of the experimental  $\theta$ (SF) values around the fitting curve, as confirmed by the general reductions of the corresponding RMSE, whose values never exceeded  $0.030 \text{ cm}^3 \cdot \text{cm}^{-3}$  for coarse-textured soils and  $0.053 \text{ cm}^3 \cdot \text{cm}^{-3}$  for fine-textured soils. For the latter, it was also observed that at the highest SF, significant variations of  $\theta$  were associated with limited changes in the scaled frequency as a consequence of the effects of shrinkage processes on soil dielectric permittivity and then on the resonant frequency detected by the sensor, confirming that capacitance sensors are influenced by properties of the soil-water system around the access tube and not only by the changes in the soil water content. To exclude the effects of soil bulk density on the soil water content, it was suggested to represent the sensor scaled frequency as a function of  $U$  rather than volumetric  $\theta$ , and thus to investigate the consequences of soil shrinkage processes on SF at the same time.

The experimental results showed that the values of SF rapidly increased at increasing  $U$ , in correspondence with the residual phase of the shrinking process (constant bulk density), became approximately constant during the normal phase of the shrinking process, in which bulk density is a function of the soil water content. In other terms, at a relatively high  $U$ , it was observed that the variations in the soil water content were in whole or in part compensated by the changes of soil bulk density so that the final scaled frequency measured by the sensor was approximately constant.

When calibrating FDR sensors on shrinking/swelling clay soils, it is then necessary to determine the soil shrinkage characteristic curve whose knowledge, associated with the sensor calibration equation expressed as  $U(\text{SF})$ , allows determination of the volumetric water content. Further investigations are, however, necessary to identify how the soil shrinkage characteristic curve can be introduced in the sensor calibration equation in terms of  $\theta(\text{SF})$  and to verify the possibility of indirect estimation of the calibration equation parameters on the basis of easy-to-measure soil physical variables.

## Acknowledgments

The research was cofinanced from Ministero dell'Istruzione, dell'Università e della Ricerca (<http://www.miur.it>) under the Project PRIN 2010-2011 and Università degli Studi di Palermo under the Project FFR 2012, both coordinated by G. Provenzano. The contribution to the manuscript has to be shared among the authors as the following: experimental setup, data processing, and final revision of the text have to be divided equally between the authors. Field data collection was cared for by G. Rallo. The text was written by G. Rallo and G. Provenzano.

## References

- Boden, A. G. (1994). *Bodenkundliche Kartieranleitung*, E. Schweizerbart'sche Verlagsbuchhandlung, Stuttgart, Germany.
- Bronswijk, J. J. B. (1990). "Shrinkage geometry of a heavy clay soil at various stresses." *Soil Sci. Soc. Am. J.*, **54**(5), 1500–1502.
- Burgess, P. J., Reinhard, B. R., and Pasturel, P. (2006). "Compatible measurements of volumetric soil water content using a neutron probe and Diviner 2000 after field calibration." *Soil Use Manage.*, **22**(4), 401–404.
- Cammalleri, C., Rallo, G., Agnese, C., Ciraolo, G., Minacapilli, M., and Provenzano, G. (2013). "Combined use of eddy covariance and sap flow techniques for partition of ET fluxes and water stress assessment in an irrigated olive orchard." *Agric. Water Manage.*, **120**, 89–97.
- Cavazza, L. (2005). *Terreno agrario: Il comportamento fisico*, Reda Editore, Italian.
- Crescimanno, G., and Provenzano, G. (1999). "Soil shrinkage characteristic in clay soils: Measurement and prediction." *Soil Sci. Soc. Am. J.*, **63**(1), 25–32.
- Davood, N. K., Shorafa, M., and Heidari, A. (2012). "Estimating soil water content from permittivity for different mineralogies and bulk densities." *Soil Sci. Soc. Am. J.*, **76**(4), 1149–1158.
- Evett, S. R., Heng, L. K., Moutonnet, P., and Nguyen, M. L. (2008). *Field estimation of soil water content: A practical guide to methods, instrumentation, and sensor technology*, S. R. Evett, L. K. Heng, P. Moutonnet, and M. L. Nguyen, eds., International Atomic Energy Agency, Vienna, Austria, 123–129.
- Evett, S. R., Ruthardt, B., Kottkamp, S., Howell, T., Scheneider, A., and Tolk, J. (2002). "Accuracy and precision of soil water measurements by neutron, capacitance and TDR methods." *Proc., 17th World Congress of Soil Science*, Thailand.
- Evett, S. R., Schwartz, R. C., Mazahreh, N., Jitan, M., and Shaqir, I. M. (2011). "Soil water sensors for irrigation scheduling: Can they deliver a management allowed depletion?" *Acta Horticulturae. Proc., Int. Symp. Olive Irrigation and Oil Quality*, Nazareth, Israel, Vol. 888, 231–237.
- Evett, S. R., and Steiner, J. L. (1995). "Precision of neutron scattering and capacitance type soil water content gauges from field calibration." *Soil Sci. Soc. Am. J.*, **59**(4), 961–968.
- Evett, S. R., Tolk, J. A., and Howell, T. A. (2006). "Soil profile water content determination: Sensor accuracy, axial response, calibration, temperature dependence, and precision." *Vadose Zone J.*, **5**(3), 894–907.
- Fares, A., and Alva, A. K. (2000). "Evaluation of capacitance probes for optimal irrigation of citrus through soil moisture monitoring in an Entisol profile." *Irrig. Sci.*, **19**(2), 57–64.
- Fares, A., Buss, P., Dalton, M., El-Kadi, A. I., and Parsons, L. R. (2004). "Dual field calibration of capacitance and neutron sensors in a shrinking-swelling clay soil." *Vadose Zone J.*, **3**(4), 1390–1399.
- Franzmeier, D. P., and Ross, S. J. (1968). "Soil swelling: Laboratory measurement and relation to other soil properties." *Soil Sci. Soc. Am. Proc.*, **32**(4), 573–577.
- Gabriel, J. L., Lizaso, J. I., and Quemada, M. (2010). "Laboratory versus field calibration of capacitance probes." *Soil Sci. Soc. Am. J.*, **74**(2), 593–601.
- Gardner, C. M. K., Dean, T. J., and Cooper, J. D. (1998). "Soil water content measurement with a high-frequency capacitance sensor." *J. Agric. Eng. Res.*, **71**(4), 395–403.
- Geesing, D., Bachmaier, M., and Schmidhalter, U. (2004). "Field calibration of a capacitance soil water probe in heterogeneous fields." *Aust. J. Soil Res.*, **42**(3), 289–299.
- Gong, Y. S., Cao, Q. H., and Sun, Z. J. (2003). "The effects of soil bulk density, clay content and temperature on soil water measurement using time domain reflectometry." *Hydrol. Processes*, **17**(18), 3601–3614.
- Grossman, R. B., Brasher, B. R., Franzmeier, D. P., and Walker, J. L. (1968). "Linear extensibility as calculated from natural-clod bulk density measurements." *Soil Sci. Soc. Am. Proc.*, **32**(4), 570–573.
- Groves, S. J., and Rose, S. C. (2004). "Calibration equations for Diviner 2000 capacitance measurements of volumetric soil water content of six soils." *Soil Use Manage.*, **20**(1), 96–97.
- Haberland, J., Gálvez, R., Kremer, C., and Carter, C. (2014). "Laboratory and field calibration of the Diviner 2000 probe in two types of soil." *J. Irrig. Drain. Eng.*, **10.1061/(ASCE)IR.1943-4774.0000687**, 04014004.

- Hignett, C., and Evett, S. (2008). "Direct and surrogate measures of soil water content." *Field estimation of soil water content: A practical guide to methods, instrumentation, and sensor technology*, S. R. Evett, L. K. Heng, P. Moutonnet, and M. L. Nguyen, eds., International Atomic Energy Agency, Vienna, Austria.
- Lukanu, G., and Savage, M. J. (2006). "Calibration of a frequency-domain reflectometer for determining soil-water content in a clay loam soil." *Water SA*, 32(1), 37–42.
- Malicki, M. A., Plagge, R., and Roth, C. H. (1996). "Improving the calibration of dielectric TDR soil moisture determination taking into account the solid soil." *Eur. J. Soil Sci.*, 47(3), 357–366.
- Mazahrih, N. Th., Katbeh-Bader, N., Evett, S. R., Ayars, J. E., and Trout, T. J. (2008). "Field calibration accuracy and utility of four down-hole water content sensors." *Vadose Zone J.*, 7(3), 992.
- Mead, R. M., Ayars, J. E., and Liu, J. (1995). "Evaluating the influence of soil texture, bulk density and soil water salinity on a capacitance probe calibration." *Proc., ASAE Summer Meeting*, Chicago.
- Morgan, K. T., Parsons, L. R., Wheaton, T. A., Pitts, D. J., and Obreza, T. A. (1999). "Field calibration of a capacitance water content probe in fine sand soils." *Soil Sci. Soc. Am. J.*, 63(4), 987–989.
- Pagliai, M. (1998). *Metodi di analisi fisica del suolo*, Editore Franco Angeli, Milan, (in Italian).
- Paltineanu, I. C. (2014). "On the importance of international standardization of methodologies and techniques for laboratory and field calibration of soil water measurement sensors based on capacitance, impedance, and TDT." *Transactions of the 4th Int. Symp. on Soil Water Measurement Using Capacitance, Impedance and Time Domain Transmission*, PALTIN International, Montreal, QC, Canada.
- Paltineanu, I. C., and Starr, J. L. (1997). "Real-time soil water dynamics using multisensor capacitance probes: Laboratory calibration." *Soil Sci. Soc. Am. J.*, 61(6), 1576–1585.
- Paraskevas, C., Georgiou, P., Ilias, A., Panoras, A., and Babajimopoulos, C. (2012). "Calibration equations for two capacitance water content probes in a Lysimeter field." *Int. Agrophys.*, 26(3), 285–293.
- Parker, J. C., Amos, D. F., and Kaster, D. L. (1977). "An evaluation of several methods of estimating soil volume change." *Soil Sci. Soc. Am. J.*, 41(6), 1059–1064.
- Polyakov, V., Fares, A., and Ryder, M. H. (2005). "Calibration of a capacitance system for measuring water content of tropical soil." *Vadose Zone J.*, 4(4), 1004–1010.
- Provenzano, G., Tarquis, A. M., and Rodriguez-Sinobas, L. (2013). "Soil and irrigation sustainability practices." *Agric. Water Manage.*, 120(31), 1–4.
- Rallo, G., Agnese, C., Minacapilli, M., and Provenzano, G. (2012). "Comparison of SWAP and FAO agro-hydrological models to schedule irrigation of wine grape." *J. Irrig. Drain. Eng.*, 10.1061/(ASCE)IR.1943-4774.0000435, 581–591.
- Rallo, G., Baiamonte, G., Manzano Juárez, J., and Provenzano, G. (2014). "Improvement of FAO-56 model to estimate transpiration fluxes of drought tolerant crops under soil water deficit: Application for olive groves." *J. Irrig. Drain. Eng.*, 10.1061/(ASCE)IR.1943-4774.0000693, A4014001.
- Rallo, G., and Provenzano, G. (2014). "Discussion of 'Laboratory and field calibration of the Diviner 2000 probe in two types of soil' by J. Haberland, R. Gálvez, C. Kremer, and C. Carter." *J. Irrig. Drain. Eng.*, 10.1061/(ASCE)IR.1943-4774.0000856, 07014063.
- Robinson, D. A., et al. (2008). "Soil moisture measurement for ecological and hydrological watershed-scale observatories: A review." *Vadose Zone J.*, 7(1), 358–389.
- Sentek Environmental Technologies. (2001). *Calibration of the Sentek Pty Ltd soil moisture sensors*, Stepney, Australia.
- Soil Survey Division Staff. (1993). *Soil survey manual*, U.S. Dept. of Agriculture, Washington, DC.
- SYSTAT 13 [Computer software]. Evanston, IL, SYSTAT.